PCCP

COMMUNICATION

View Article Online
View Journal | View Issue

Cite this: *Phys. Chem. Chem. Phys.*, 2014, **16**, 26691

Received 14th August 2014,
Accepted 1st September 2014

DOI: 10.1039/c4cp03642e

www.rsc.org/pccp

Infrared detection of $(H_2O)_{20}$ isomers of exceptional stability: a drop-like and a face-sharing pentagonal prism cluster†

Christoph C. Pradzynski,[a] Christoph W. Dierking,[a] Florian Zurheide,[a] Richard M. Forck,[a] Udo Buck,[b] Thomas Zeuch*[a] and Sotiris S. Xantheas*[c]

Water clusters with internally solvated water molecules are widespread models that mimic the local environment of the condensed phase. The appearance of stable $(H_2O)_n$ cluster isomers having a fully coordinated interior molecule has been theoretically predicted to occur around the n = 20 size range. However, our current knowledge about the size regime in which those structures become energetically more stable has remained hypothetical from simulations in lieu of the absence of precisely size-resolved experimental measurements. Here we report size and isomer selective infrared (IR) spectra of $(H_2O)_{20}$ clusters tagged with a sodium atom by employing IR excitation modulated photoionization spectroscopy. The observed absorption patterns in the OH stretching region are consistent with the theoretically predicted spectra of two structurally distinct isomers of exceptional stability: a drop-like cluster with a fully coordinated (interior) water molecule and an edge-sharing pentagonal prism cluster in which all atoms are on the surface. The drop-like structure is the first experimentally detected water cluster exhibiting the local connectivity found in liquid water.

Water clusters are of relevance to many fields of science like atmospheric and astrophysical chemistry[1,2] and have been reported to be trapped inside inorganic crystals,[3] polymers[4] and in crystal structures of hydrophobic proteins.[5] In an aqueous solution the chemical reactivity is coupled to the subtle balance between the solvent–solute and solvent–solvent interactions that ultimately control the fleeting hydrogen bonding network. Water clusters provide a medium for probing the underlying solvent–solvent interactions in those aqueous environments and quantifying the properties of the hydrogen bonding interactions at the molecular level. Contrary to the fully connected network in liquid water, the structures of the first few water clusters exhibit arrangements in which all atoms are on the surface of the cluster,[6–12] a consequence of the need to maximize the number of hydrogen bonds in combination with the large surface-to-volume ratio that is characteristic of a small water cluster. The emergence and isomerism of three-dimensional, neutral water clusters in the size range of 6 to 10 molecules is by now understood in great detail.[8,9,11,13–16] However, all water molecules in these clusters are under-coordinated, having less than four neighbors, the number found on the average in bulk water. Previous theoretical studies[17,18] have identified a cluster size regime starting at around 17 molecules for which the transition between the "all-surface" to "interior" structures, *viz.* the appearance of stable cluster isomers with an interior, fully coordinated water molecule, may occur. The fact that experimental, size-resolved probes of either the infrared (IR) "fingerprint" region (3000 to 4000 cm^{-1})[14,15,19–21] or the broadband rotational spectrum[11,22] have so far been limited to smaller sized clusters, has prevented the direct experimental probing of this important size regime. Therefore, these previous theoretical studies have been unchallenged by experiments, in contrast to the case of aqueous ionic clusters.[23,24] Here we report size and isomer selective infrared (IR) spectra of $(H_2O)_{20}$ clusters tagged with a sodium atom in the OH stretching region. The ensuing analysis will demonstrate that the isomer composition of this water cluster size is consistent with predictions of high level electronic structure calculations.

Hydrogen bonding interactions of fully coordinated water molecules that are characteristic of condensed environments consist of arrangements in which each molecule, on the average, both donates and accepts two hydrogen bonds (double donor–double acceptor configuration: DDAA).[25] This connectivity leads to a complex, three-dimensional network of four-coordinated water molecules that is transient in the liquid[26] and static in solid water.[27] Therefore, a special interest arises in identifying the emergence of water clusters which posses fully coordinated

[a] *Institut für Physikalische Chemie, Universität Göttingen, Tammannstr. 6, 37077 Göttingen, Germany. E-mail: tzeuch1@gwdg.de*
[b] *Max-Planck-Institut für Dynamik und Selbstorganisation, Am Faßberg 17, 37077 Göttingen, Germany*
[c] *Physical Sciences Division, Pacific Northwest National Laboratory, 902 Battelle Boulevard, P.O. Box 999, MS K1-83, Richland, WA 99352, USA. E-mail: Sotiris.Xantheas@pnnl.gov*

† Electronic supplementary information (ESI) available. See DOI: 10.1039/c4cp03642e

water molecules. In this context, the neutral $(H_2O)_{20}$ clusters have previously served as a reference system for benchmarking theoretical methods, see ref. 28–31 and references cited therein. Additional reasons for studying clusters of this size is their potential connection to the "magic number" protonated water clusters,[23,29,32] the dodecahedral cage network of one of its families of isomers that is the building block of the structure I (sI) clathrate lattices[33,34] as well as their use as a model for cloud droplets in atmospheric reactions.[2]

The frequencies of the OH stretch oscillators can be used as a sensitive probe of the strength of the underlying hydrogen bonds: the stronger the intermolecular bond, the weaker the corresponding O–H covalent bond is, which leads to sizeable red shifts of such oscillators in the IR spectrum.[35] To this end, vibrational spectroscopy of size-selected, neutral clusters is a powerful tool that probes the characteristic absorption patterns of the hydrogen bonded OH stretching vibrations[16] which, in conjunction with theoretical calculations, can be used to assign the underlying hydrogen bonded network *via* the "structural-spectral correspondence" principle.[36] By applying such an experimental approach, the emergence of four-coordinated water molecules[37] for $n > 18$ and the onset of crystallinity in larger clusters[38] have been characterized in previous experimental studies. We have recently reported an experimental approach, which allows to record precisely size-resolved infrared spectra in the OH stretching region of sodium tagged, neutral water clusters.[38,39] The viability of the new method for arriving at structure assignments was indicated for sizes above $n = 20$,[39] but not rigorously proven. In the present work, the approach is further refined and coupled with first principles electronic structure calculations to assign the measured spectra for $n = 20$.

In the experiment, a molecular beam containing the clusters is formed in a skimmed supersonic expansion. The clusters are then doped with a single sodium atom in a pick-up cell and subsequently irradiated with IR photons inducing a signal enhancement to the UV photoionization, which is delayed by 80 ns. A single scan of the OH stretch region (2850 to 3800 cm^{-1}) with a tuneable IR laser system provides simultaneously measured, size-resolved IR spectra for the complete cluster size distribution. The problem of UV photon induced fragmentation can be suppressed already in small clusters[40,41] due to the special ionization mechanism of sodium doped, hydrogen bonded clusters.[42] For larger clusters ($n > 18$) a spectral contamination by the sodium atom was not observed.[38] In this study we used neon (Ne) and argon (Ar) instead of helium as seeding gas. The reason is the better suitability of Ne and Ar expansions to cool water clusters[41] and to relax them in their thermodynamical minima.[43] Further experimental details are found in[38,40,42] and in the ESI,† in which also the reproducibility of the main features in the presented spectra is shown.

The electronic structure calculations were performed at the second-order Møller–Plesset perturbation theory (MP2) level of theory with Dunning's augmented, correlation-consistent basis sets (aug-cc-pVnZ)[44] of double through quadruple (n = D, T, Q) zeta quality allowing for the extrapolation of the energetics at the Complete Basis Set (CBS) limit (see ref. 28 for details). Geometries were optimized with the double and triple zeta basis sets whereas single point energies were obtained with the larger quadruple zeta set at the triple zeta geometries. Harmonic vibrational spectra and subsequent zero-point energy (ZPE) corrections are obtained with the aug-cc-pVDZ basis set. These calculation have been conducted on isomer B in the present study, the results for isomers A and C were taken from previous work.[28] All electronic structure calculations were carried out with the NWChem suite of codes.[45]

The structures, relative energetics and corresponding IR spectra of the various families of $(H_2O)_{20}$ minima from first principles have been reported in previous theoretical studies.[17,18,28–31] A "family" of isomers denotes clusters with the same oxygen network differing only in the position of the hydrogen atoms according to the Bernal–Fowler ice rules.[46] The stability of the edge-sharing pentagonal prisms, first suggested using classical force fields,[47] was confirmed as the most stable family of minima from high level electronic structure calculations. The lowest isomer of this family[28] is shown in Fig. 1 (isomer A) together with the predicted infrared spectrum in the OH stretching region. It is a highly symmetric structure (as regards the oxygen atom network) and features in total eight water molecules in DDAA configurations, which are all placed at the surface of the cluster. Additionally, there are six water molecules having a single donor–double acceptor motif (DAA), which show a characteristic single peak in the most red-shifted part of the OH stretching spectrum.

An energetically competitive, (*cf.* Table 1) drop-like[31] isomer of $(H_2O)_{20}$ is also considered (isomer B in Fig. 1). This isomer features a total of six fully coordinated and interconnected water molecules, five of which are on the surface and one DDAA-like fragment at the center of the cluster. Four out of the former five surface fragments are hydrogen bonded to the latter interior one. The surface of isomer B consists of four 4-, six 5- and two 6-member rings. Interconnected 4- and 6-member rings cover roughly one half of the surface area, whereas interconnected 5-member rings cover the other half. The most red-shifted part in the "fingerprint" OH stretching region of the IR spectra provides a definitive feature used for the structural identification of isomer B. There exists a characteristic pattern of seven DAA oscillators which arrange in three peaks of different intensities caused by the different environment. The dominant band is predicted to be more red-shifted than the corresponding single peak found in the edge-sharing pentagonal prism, isomer A. Other families of $(H_2O)_{20}$ isomers that have been discussed in the past, like those of the facesharing pentagonal prisms (isomer C in Fig. 1), the fused cubes, and the dodecahedron are predicted to be significantly less stable[28] (*cf.* Table 1). Note that the ordering of the isomers in the various families does not change upon either increasing the basis set to CBS or including harmonic ZPE corrections, as seen from Table 1. The small energy difference between isomers A and B, obtained at the highest level of electronic structure theory considered in this study including ZPE corrections, suggests that we expect only two different cluster networks to contribute to the IR spectrum in the OH stretching region of $(H_2O)_{20}$, each showing one characteristic feature in the region of DAA oscillators.

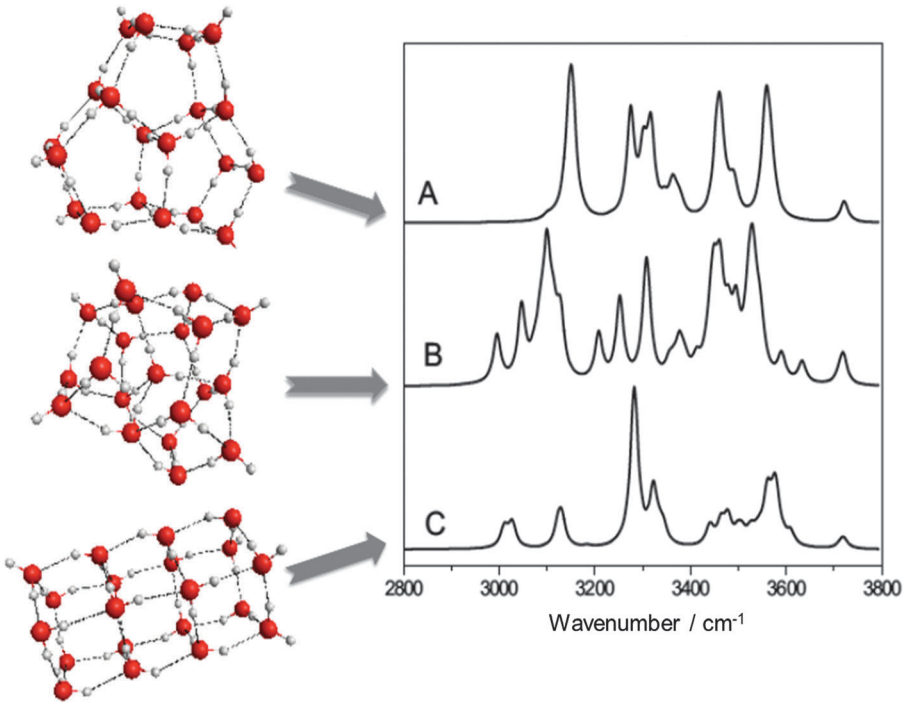

Fig. 1 The most stable isomers of $(H_2O)_{20}$, as identified in this and previous work[28,31] and their predicted IR spectra in the OH stretch region. (A) Edge-sharing pentagonal prism, (B) drop-like, (C) face-sharing pentagonal prism.

In Fig. 2 the IR spectrum of the sodium tagged $(H_2O)_{20}$ cluster is shown together with simultaneously measured ones of cluster sizes n = 19, 21. Here, we have to concentrate on the marked region of the most red shifted part of the spectrum of the DAA stretch motion. Only for the $Na(H_2O)_{20}$ cluster we observe a characteristic double peak, which corresponds to the specific DAA features of isomers A and B. In the upper panel of Fig. 3 the experimental IR spectrum generated in the Ne expansions is compared with a simulated one, in which the ratio of isomer A (35%) and B (65%) is chosen such that similar intensities for the characteristic DAA peaks are obtained. Note that the frequencies in all simulated spectra are scaled by 0.96 to account for the harmonic approximation. The summed-up spectrum agrees well with the experimentally observed absorption pattern over the complete OH stretching region. In the experiment the strong double-donor single-acceptor (DDA) modes appear at slightly lower frequencies (3400 cm^{-1}) compared to the predicted harmonic spectra. Such deviations are expected due to the uniform scaling of the harmonic frequencies.[18] The assignment

Table 1 MP2 binding energies (in kcal mol^{-1} with respect to 20 isolated water molecules) with different basis sets including Complete Basis Set (CBS) limit estimates for the various isomers of $(H_2O)_{20}$. Zero-point energy (ZPE) corrections are estimated with the aug-cc-pVDZ basis set

	Edge-sharing[a]	Drop-like	Face-sharing[a]		
Basis set	Isomer A	Isomer B	Isomer C	Fused cubes[a]	Dodeca-hedron[a]
aug-cc-pVDZ	−224.5	−224.2	−223.1	−222.4	−212.0
aug-cc-pVTZ	−220.3	−219.1	−218.5	−217.9	−209.3
aug-cc-pVQZ	−219.0	−217.5	−216.6	−215.3	−205.2
CBS	***−217.9***	***−216.3***	***−215.0***	***−212.6***	***−200.1***
CBS (ZPE)	***(−163.1)***	***(−162.6)***	***(−160.1)***	***(−157.3)***	***(−147.9)***

[a] From ref. 28.

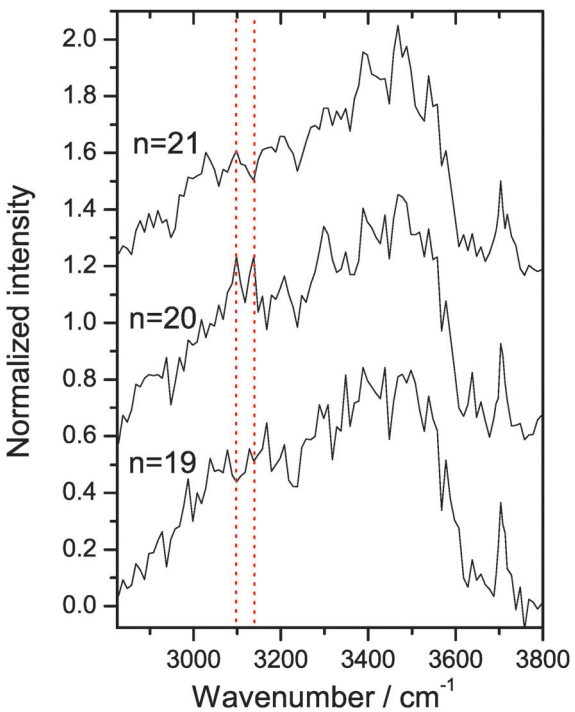

Fig. 2 Comparison of simultaneously recorded, maximum intensity normalized OH stretch spectra of $Na(H_2O)_{19,20,21}$. 0.6 offset for n = 20, 1.2 offset for n = 21. Expansion conditions: water at 373 K (1.0 bar) in Ne at (2.3 ± 0.1) bar stagnation pressure, nozzle temperature 383 to 433 K, photoionization at 388 nm or in one case at 360 nm.

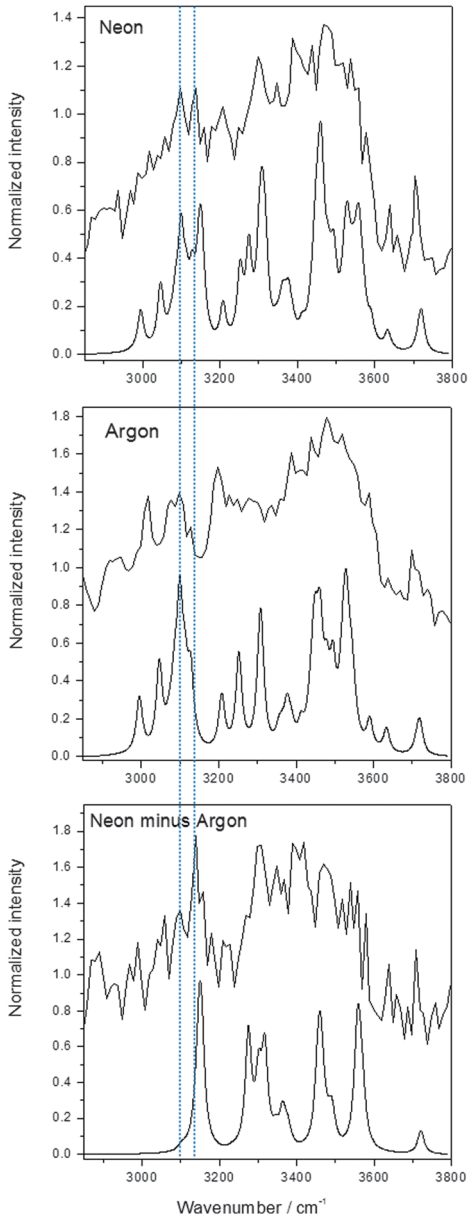

Fig. 3 Comparison of experiment with theory. Maximum intensity normalized OH stretch spectra of $Na(H_2O)_{20}$ recorded in Ne (upper panel, offset 0.4) and Ar (middle panel, offset 0.8) seeded expansions are compared with simulated spectra of a mixture of isomer A (35%) and isomer B (65%). Expansion conditions: water at 323 to 353 K (0.12 to 0.47 bar) in Ar at 1.0 to 1.7 bar stagnation pressure, see Fig. 2 for Ne-seeded expansions and supplement for more details. Photoionization was performed at 360 or 388 nm.

of the DAA double peak to isomers A and B would further become more definitive upon depopulation of one of the isomers in the experiment. This was indeed achieved by changing the seed gas and stagnation pressure. The middle panel of Fig. 3 shows the spectrum obtained in Ar-seeded expansions, compared to the predicted IR spectrum of isomer B alone. Again, the experimentally observed OH stretch absorption pattern is consistent with the theoretical prediction thus providing further credence to the structural assignment. The DAA peak characteristic to isomer A is completely suppressed in this experiment and the structure sensitive DAA region agrees well with the predicted absorption pattern of isomer B. Both experiment and calculation consistently show the separation of DAA oscillators appearing below 3180 cm^{-1} and DDAA oscillators appearing above 3200 cm^{-1}. The high intensity of the low-lying DDAA oscillator is probably caused by a Fermi resonance with the overtone of the OH bending motion appearing around 3200 cm^{-1}, as recently shown by Suhm and co-workers for small water clusters in spontaneous Raman scattering experiments.[48] Similar to the expansion with Ne as seed gas, the strong DDA features appear at 3400 cm^{-1} indicating that the calculated DDA part of the spectrum is a bit too compressed. The absence of isomer A in the Ar-seeded expansions could indicate a slightly higher stability of isomer B. However, also a kinetic effect seems plausible, which would indicate a better relaxation of clusters to the thermodynamic minima in the Ne experiment. The cluster temperatures are estimated to be around 100 K for the Ne-seeded expansions; the Ar-seeded experiment is expected to produce colder clusters (see discussion in ref. 39 for temperature estimates). The isolation of isomer B achieved in the Ar-seeded expansion allows for an additional consistency test of our spectral assignments, facilitated by subtracting the spectrum recorded using Ar as seed gas from the one taken in the Ne-seeded expansion. Ideally, this difference spectrum, shown in the lower panel of Fig. 3, should reveal the characteristic absorption pattern of isomer A: the single DAA peak around 3140 cm^{-1} and a broad intensity gap between this peak and the absorption maximum of the DDAA oscillators, predicted to be around 3300 cm^{-1}. This highly characteristic feature is indeed found in the difference spectrum, with the gap being larger than predicted from the harmonic frequencies. Again, the (anharmonic) effect of the Fermi resonance with the overtone of the OH bending motion might explain this observation. Here, the close lying DDAA oscillators seem to be blue-shifted, away from the resonance around 3200 cm^{-1}, as found for the in-phase, hydrogen-bonded OH stretching motion in the cyclic water pentamer.[48] The consistency of the difference spectrum with the calculated one of isomer A alone suggests that indeed the isomer families A and B dominate the isomer composition of $Na(H_2O)_{20}$ in the experiments. Since isomer A has a highly symmetric oxygen network, the experimental IR spectrum should be sensitive to the influence of our sodium atom tag. We analyzed this effect and found only a weak influence on the general IR absorption pattern for sodium doped versions of isomer A (see ESI†). However, satellite peaks around the single DAA peak are predicted. Such spiky features in the DAA region are found in the Ne seed gas experiment (and in the difference spectrum), in which isomer A is present (see Fig. 3). The simulations further indicate that DDAA oscillators are slightly blue-shifted in the Na tagged cluster. This effect would be an alternative explanation for the relatively large absorption gap between the DAA and DDAA features of isomer A and the missing gap between DDAA and DDA oscillators in all spectra.

In the discussion above we have presented theoretical and experimental evidence that isomers A and B, the edge-sharing pentagonal prism and a drop-like structure, are the most stable

configurations of $(H_2O)_{20}$. The assignment is anchored on the energy ranking based on high-level first principles electronic structure calculations (*cf.* Table 1) and the consistency between isomer selective, experimental IR spectra and theoretical predictions (Fig. 3). With regard to the ongoing tedious experimental and theoretical exploration of the $(H_2O)_6$ structures, initiated over almost two decades ago,[8,11,14,15,49] the current study represents a significant step towards expanding the size regime of neutral water clusters that can be probed experimentally. The drop like cluster is the first experimentally detected cluster with a fully coordinated interior water molecule featuring the local environment in liquid water. This feature was theoretically expected to occur first in water clusters with an odd number of water molecules[17] starting with $n = 17$. The similarity of the spectral envelope for $n = 19$, 20, 21 (see Fig. 2) may indicate that the neighboring cluster sizes of $n = 20$ also feature large fractions of isomers with interior water molecules. The DAA region and the corresponding free OH stretch features are similar for $n = 21$ in Fig. 2 and the spectrum assigned to the drop like isomer of $n = 20$ in the middle panel of Fig. 3. We note that a centred dodecahedron was discussed as global minimum for $n = 21$[17] and that one half of the surface of isomer B shows this topology of interconnected five member rings. In future the approach presented in this work may allow for further structural assignments of water clusters. However, at the moment it is not clear whether one or two energetically distinguished isomer families as found for $n = 20$ exist for water clusters containing more than 20 water molecules.[39]

Acknowledgements

TZ acknowledges the ongoing support of Prof. Martin Suhm and funding by the DFG (GRK 782, grant ZE 890-1-1/2). SSX acknowledges support from the US Department of Energy, Office of Basic Energy Sciences, Division of Chemical Sciences, Geosciences and Biosciences. Pacific Northwest National Laboratory (PNNL) is a multiprogram national laboratory operated for DOE by Battelle. This research used resources of the National Energy Research Scientific Computing Center, which is supported by the Office of Science of the U.S. Department of Energy under Contract No. DE-AC02-05CH11231.

References

1 L. Delzeit and D. Blake, *J. Geophys. Res.: Planets*, 2001, **106**, 33371–33379.
2 Q. Shi, S. D. Belair, J. S. Francisco and S. Kais, *Proc. Natl. Acad. Sci. U. S. A.*, 2003, **100**, 9686–9690.
3 W. B. Blanton, S. W. Gordon-Wylie, G. R. Clark, K. D. Jordan, J. T. Wood, U. Geiser and T. J. Collins, *J. Am. Chem. Soc.*, 1999, **121**, 3551–3552.
4 J. Wu and J.-Q. Liu, *Inorg. Chim. Acta*, 2013, **402**, 20–24.
5 M. M. Teeter, *Proc. Natl. Acad. Sci. U. S. A.*, 1984, **81**, 6014–6018.
6 N. Pugliano and R. J. Saykally, *Science*, 1992, **257**, 1937–1940.
7 R. N. Pribble and T. S. Zwier, *Science*, 1994, **265**, 75–79.
8 K. Liu, M. J. Brown, C. Carter, R. J. Saykally, J. K. Gregory and D. C. Clary, *Nature*, 1996, **381**, 501–503.
9 C. J. Gruenloh, J. R. Carney, C. A. Arrington, T. S. Zwier, S. Y. Fredericks and K. D. Jordan, *Science*, 1997, **276**, 1678–1681.
10 K. Nauta and R. E. Miller, *Science*, 2000, **287**, 293–295.
11 C. Pérez, M. T. Muckle, D. P. Zaleski, N. A. Seifert, B. Temelso, G. C. Shields, Z. Kisiel and B. H. Pate, *Science*, 2012, **336**, 897–901.
12 J. D. Cruzan, L. B. Braly, K. Liu, M. J. Brown, J. G. Loeser and R. J. Saykally, *Science*, 1996, **271**, 59–61.
13 U. Buck, I. Ettischer, M. Melzer, V. Buch and J. Sadlej, *Phys. Rev. Lett.*, 1998, **80**, 2578–2581.
14 C. Steinbach, P. Andersson, M. Melzer, J. K. Kazimirski, U. Buck and V. Buch, *Phys. Chem. Chem. Phys.*, 2004, **6**, 3320–3324.
15 E. G. Diken, W. H. Robertson and M. A. Johnson, *J. Phys. Chem. A*, 2004, **108**, 64–68.
16 U. Buck and F. Huisken, *Chem. Rev.*, 2000, **100**, 3863–3890.
17 B. Hartke, *Phys. Chem. Chem. Phys.*, 2003, **5**, 275–284.
18 A. Lagutschenkov, G. S. Fanourgakis, G. Niedner-Schatteburg and S. S. Xantheas, *J. Chem. Phys.*, 2005, **122**, 194310.
19 F. Huisken, M. Kaloudis and A. Kulcke, *J. Chem. Phys.*, 1996, **104**, 17–25.
20 S. Hirabayashi and K. M. T. Yamada, *J. Chem. Phys.*, 2005, **122**, 244501.
21 J. Ceponkus, P. Uvdal and B. Nelander, *J. Phys. Chem. A*, 2012, **116**, 4842–4850.
22 C. Pérez, S. Lobsiger, N. A. Seifert, D. P. Zaleski, B. Temelso, G. C. Shields, Z. Kisiel and B. H. Pate, *Chem. Phys. Lett.*, 2013, **571**, 1–15.
23 J.-W. Shin, N. I. Hammer, E. G. Diken, M. A. Johnson, R. S. Walters, T. D. Jaeger, M. A. Duncan, R. A. Christie and K. D. Jordan, *Science*, 2004, **304**, 1137–1140.
24 K. R. Asmis and D. M. Neumark, *Acc. Chem. Res.*, 2012, **45**, 43–52.
25 S. S. Xantheas, *Chem. Phys.*, 2000, **258**, 225–231.
26 T. Steinel, J. B. Asbury, J. Zheng and M. D. Fayer, *J. Phys. Chem. A*, 2004, **108**, 10957–10964.
27 N. Bjerrum, *Science*, 1952, **115**, 385–390.
28 G. S. Fanourgakis, E. Aprà and S. S. Xantheas, *J. Chem. Phys.*, 2004, **121**, 2655–2663.
29 S. S. Xantheas, *Can. J. Chem. Eng.*, 2012, **90**, 843–851.
30 P. Parkkinen, S. Riikonen and L. Halonen, *J. Phys. Chem. A*, 2013, **117**, 9985–9998.
31 J. P. Furtado, A. P. Rahalkar, S. Shanker, P. Bandyopadhyay and S. R. Gadre, *J. Phys. Chem. Lett.*, 2012, **3**, 2253–2258.
32 M. Miyazaki, A. Fujii, T. Ebata and N. Mikami, *Science*, 2004, **304**, 1134–1137.
33 E. D. Sloan, *Clathrate Hydrates of Natural Gases*, Marcek Dekker, New York, 2nd edn, 1998.
34 S. Yoo, M. V. Kirov and S. S. Xantheas, *J. Am. Chem. Soc.*, 2009, **131**, 7564–7566.
35 R. M. Badger, *J. Chem. Phys.*, 1934, **2**, 128–131.
36 C. J. Burnham, S. S. Xantheas, M. A. Miller, B. Applegate and R. E. Miller, *J. Chem. Phys.*, 2002, **117**, 1109–1122.

37 T. Hamashima, K. Mizuse and A. Fujii, *J. Phys. Chem. A*, 2011, **115**, 620–625.
38 C. C. Pradzynski, R. M. Forck, T. Zeuch, P. Slavicek and U. Buck, *Science*, 2012, **336**, 1529–1532.
39 U. Buck, C. C. Pradzynski, T. Zeuch, J. M. Dieterich and B. Hartke, *Phys. Chem. Chem. Phys.*, 2014, **16**, 6859–6871.
40 R. M. Forck, C. C. Pradzynski, S. Wolff, M. Oncak, P. Slavicek and T. Zeuch, *Phys. Chem. Chem. Phys.*, 2012, **14**, 3004–3016.
41 R. M. Forck, J. M. Dieterich, C. C. Pradzynski, A. L. Huchting, R. A. Mata and T. Zeuch, *Phys. Chem. Chem. Phys.*, 2012, **14**, 9054–9057.
42 T. Zeuch and U. Buck, *Chem. Phys. Lett.*, 2013, **579**, 1–10.
43 R. M. Young, A. A. Yandell, S. B. King and D. M. Neumark, *J. Chem. Phys.*, 2012, **136**, 094304.
44 R. A. Kendall, T. H. Dunning Jr. and R. J. Harrison, *J. Chem. Phys.*, 1992, **96**, 6796–6806.
45 M. Valiev, E. J. Bylaska, N. Govind, K. Kowalski, T. P. Straatsma, H. J. J. van Dam, D. Wang, J. Nieplocha, E. Aprà, T. L. Windus and W. A. deJong, *Comput. Phys. Commun.*, 2010, **181**, 1477–1489.
46 J. D. Bernal and R. H. Fowler, *J. Chem. Phys.*, 1933, **1**, 515–548.
47 D. J. Wales and M. P. Hodges, *Chem. Phys. Lett.*, 1998, **286**, 65–72.
48 K. E. Otto, Z. Xue, P. Zielke and M. A. Suhm, *Phys. Chem. Chem. Phys.*, 2014, **16**, 9849–9858.
49 C. J. Tainter and J. L. Skinner, *J. Chem. Phys.*, 2008, **137**, 104304.